Journal of Harbin Engineering University
ISSN: 1006-7043
Vol 47 No 02
February 2026

Shaded Dispersed Topology: An Improved PV Array Configuration for Power Enhancement under Irradiance Variations

[1.] **Kapil Khatri**, [2]**Mirza Mohammad Shadab**,
Electrical Engineering, Integral University Lucknow
Electrical Engineering, Integral University, Lucknow

Abstract: This article introduces a novel shaded dispersed topology (SDT) by using a square matrix of array size 9 using different PV modules. The concentrated partial shading in the proposed SDT arrangement is converted into dispersed shading through a total cross-tied (TCT) topology by using static reconfiguration where it does not alter the electrical connections and only the position of modules being changed for reducing the line losses. The primary objective is to alleviate partial shading losses and subsequently boost power generation and other performance parameters. Extensive simulations confirm the enhanced performance during partial shading conditions with different irradiance conditions compared to the conventional total cross-tied set up. Simulation results make a confirmatory note that the proposed novel arrangement has very few local multiple peaks, high fill factor(FF), high row current, a significant increase in array power, less mismatch power losses(MP loss) and last but not the least- the efficiency of the proposed system surpasses the traditional total cross-tied topology. The investigation assesses how well the system performs in the presence of four unique shading patterns. The proposed shaded dispersed topology demonstrates superior adaptability compared to conventional PV configurations. This unique design ensures reliability and consistency of power output under partial shading conditions.

Keywords: Shaded Dispersed Topology, total cross-tied, fill factor, mismatch power loss, partial shading condition, global peak power point.

1. Introduction:

The contemporary world has observed a significant rise in the renewable sources and request for sustainable energy sources, which have effectively taken the place of traditional energy sources on a substantial level. Renewable energy sources have become integral components of today's energy supply landscape (1). Undoubtedly, solar power stands out as the foremost and primary sustainable energy source (2). The energy produced from photovoltaic (PV) systems using sunlight not only demands minimal maintenance but is pollution free and cost efficient. A variety of commonplace uses for the energy produced by the PV technology are possible, including lighting up homes, lighting up the streets, and even supplying power to solar parking lots (3). It can also be incorporated into power infrastructure and used as an energy source in remote places that are still without connected electricity.

The effectiveness of PV modules and how well they work in use can be affected by a variety of factors and among all; partial shading is the most dominating factor (4). Partial shading is a phenomenon known as asymmetric shadowing that can be brought on by a variety of elements, including the shade cast by large objects, cloud motion, birds swooping etc. (5). Partial shadowing in a solar photovoltaic (PV) array can significantly affect how efficiently it produces electricity. In a PV array, shaded modules receive less sunlight than unshaded modules do, which affects how much power they generate. This difference has the potential to limit the array's overall output in a number of ways, including by restricting the final output current. As a result,

mismatch losses harm the PV module as a whole. In more dire circumstances, the PV cells themselves may sustain damage. A potential resolution for this issue involves the installation of a bypass diode, which would be connected at the terminal's extremities. By doing so, it can effectively safeguard the PV modules in shaded areas, preventing any potential harm.

Partial darkening causes the I-V characteristics and the P-V characteristics to have several peaks (6,7). With the numerous peaks in picture, there is a unique peak which refers to highest output power. This peak is defined as global peak power point (GPPP) and the peaks other than the maximum peaks are known as local maximum power points (LMPPs). This situation is analogous to the Elliott wave which is a combination of impulse and correction wave. The biggest problem with LMPPs is that during maximum power tracking (8,9) these LMPPs act like enemies and interrupt with the real identification of GPPP. The significant factors which decide the amount of power loss due to partial shading can be divided into 3 parts: firstly, the actual ordinate of PV modules in PVA, the second factor is the irradiance level of different modules creating a random shading pattern and lastly, the chosen array which plays a critical role because maximum power output varies with a variable PVA configuration (PVAC). Therefore, precise array usage is necessary for improved outcomes. The modules can be connected in different ways which will result into distinguished array configurations. For instance, if the modules are simply in series, then we have simple-series (SS), if they are parallel, then we have parallel (P), the twin combination of series and parallel will result into series-parallel (SP), depending upon the ties, we have total cross-tied (TCT), with bridge formation, we have bridge-link (BL) and if ties are connected such that it looks like a honey comb, then we have honey-comb (HC). All these configurations are significant in keeping the mismatch power loss within the permissible range during partial shading (10). The writers of Ref. (11) elucidated the light on the most effective arrangement for obtaining the maximum power under circumstances involving shade by examining series, series-parallel and honey-comb designs. The article's findings indicate that, in contrast to SP PVAs, TCT and BL PVACs increase reliability while reducing mismatch power losses (MP loss). The findings of logical and relative research using several PVACs, such as "SP, SS, TCT, HC, and BL," as observed under PSCs, were provided in Ref. (12). In order to more effectively evaluate and contrast the consequences of each design, the author took into account a variety of factors. The PVA setups with the names "P, SS, TCT, HC, BL, and SP" modelled and simulated under partial shading conditions of various types were shown in Ref. (13). The operational performance of each arrangement was evaluated in the article. The research outcomes validated that, when contrasted with alternative photovoltaic array setups, the TCT photovoltaic array notably amplifies the maximum global power. Thus, research to far indicate that the TCT solar array outperforms the existing configurations in terms of maximum power generation when exposed to partial shadowing. Nevertheless, when a sizable number of shaded PV modules are stacked in a single row, the TCT configuration presents a significant problem because it limits the overall output current produced by the array (14). To examine and tackle this difficulty, a number of publications have developed reconfiguration solutions for TCT arrays. By evenly dispersing the shade effects from a single row over a number of adjacent rows, these techniques aim to reduce mismatch-related losses under partial shading circumstances (15).

Reconfiguration procedures fall into two main categories: dynamic and static. As the name implies, reconfiguration technique falling in the category of dynamic involves the change in the position of PV modules by changing the electrical connection within the PVA ensuring maximum efficacy under PSCs. The authors of Ref. (16) enlightened about a special controller whose input signals were different irradiance levels and depending upon it, the controller modified the connections of PV modules and the load performed well under this dynamic reconfiguration technique. Later on, this idea was adopted to improve the efficacy of an

electric car under different working modes: starting mode, interim mode and power mode. The authors of Ref. (17) used a fuzzy logic controller to select a proper array for different irradiance levels. A set of rules based on irradiance level was defined for a particular PV array by the authors of Ref. (18). An efficient system of PV array was used by the authors of Ref. (19) for the distribution of energy on commercial basis. The best reconfiguration algorithm was optimised by the authors of Ref. (20) to get the better results under PSCs by relocating the PV modules within the PVA. This in turn improved the non-uniformity in the level of irradiance. A novel array reconfiguration algorithm was used in Ref. (21) to dominate the shading conditions. The authors of Ref. (22) have used variable switching states so that different PV modules adapt the situation accordingly under PSCs and each row current was independent of the irradiance level. The authors of Ref. (23) have used dynamic reconfiguration technique which makes the system cumbersome and uneconomical because of certain factors that include the programmable switching patterns for the PV modules in a better order to adapt the situation of PSCs, it includes the devices to react according to the shading and faulty scenarios and validation of optimal power under a complicated algorithm.

There is an advantage of static reconfiguration technique over dynamic reconfiguration technique with a unique feature of just relocating the PV modules without changing any electrical connection. This made the shading patterns to accumulate over the entire array instead of focussing on a particular part of a panel. A unique curved reconfiguration for augmenting the power under PSCs was clearly explained in Ref. (24). A novel schematic was proposed by the authors of Ref. (25) which was in the form of a square PVA of 3rd level that distributed the shading factor over the entire array resulting in the optimal global maximum power and this was compared with the conventional schematic topologies. A novel magical-rhombus PVA reconfiguration was introduced by the authors of Ref. (26) for the intensification of maximum power output. This highlighted the beauty of power loss gap under the curve of without PSC and with PSC and ensuring the least mismatch power loss. The authors of Ref. (27) proposed a twin PVA that made a usage of dispersed shading pattern spread over the entire array and improved the performance parameters.

A logical or puzzle based novel PVA was focussed by the authors of Ref. (28). To incorporate this puzzle TCT array was taken and it was expected to give better output performance in terms of global maximum power and fill factor (FF). Later on it was concluded that under PSCs, although the shading pattern was dispersed over the entire array but the pattern remained unchanged in the principal column. This decremented the total output power along with the multiple dips in the power curve plotted against the voltage curve.

To inculcate a better response in terms of performance parameters and efficiency, this research clearly focuses on a novel and command based array configuration of 9th level to get best adapted under the situation of PSCs. It uses static array reconfiguration where the positioning of modules are according to the logic without changing the arrangements electrically. The performance parameters are compared with the conventional topologies under different shading scenarios.

2. Schematic Enlightenment

2.1 Mathematical Modelling for a Photovoltaic Cell

The fundamental part that constitutes a photovoltaic array is a PV cell. The PV cell consists of a unity-diode model (2) as shown in Figure 1. The response given by PV cell can be deduced as follows:

$$I_r = I_s - I_{rs}\left(e^{\frac{q(V_r+R_{se}I_r)}{\beta kT}} - 1\right) - \left(\frac{V_r+R_{se}I_r}{R_{sht}}\right) \quad (1)$$

Where, the response current and voltage from solar cell is given by I_r and V_r respectively, the current produced by PV cell due to solar light is depicted as Is, the diode reverse saturation current is given by I_{rs}, T represents temperature of the junction, k is the Boltzmann

constant, q resembles charge on one electron, β is called diode identity constant, R_{se} is the series resistance and R_{sht} is the parallel resistance.

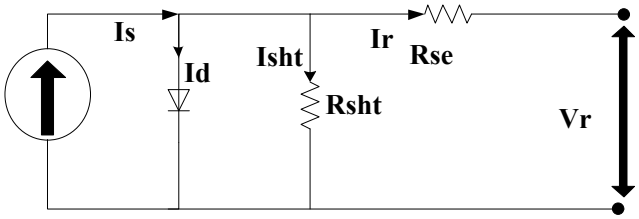

Fig.1 Equivalent circuit of a unity-diode model

3. Multiple Schemes on Photovoltaic Array

3.1 Traditional Topologies of Photovoltaic Array

There are multiple traditional topologies of PVAC's like TCT, HC, BL, SP etc. based on which, this paper clearly illustrates the results of 9 by 9 TCT. When nine columns are shunted such that each one of them consists of nine modules holding together in series, then this configuration is called 9 by 9 SP PVAC. When every column is cross-linked with the non-adjacent column, then this configuration is called 9 by 9 BL PVAC. When the structure seems to be beehive by tying up the n^{th} column with $(n+1)^{th}$ column, then it is called 9 by 9 HC PVAC. When we have series-parallel (SP) combination of different cross-ties with respect to the rows, then it is referred as a 9 by 9 TCT PVAC (29 and 30). Figure.2 shows a traditional glimpse of 9 by 9 PVACs. The rows in a TCT consists of modules where the modules itself are connected in parallel while if you look at the column, the modules are connected in series. With 9 by 9 array (means 9 rows and 9 columns), it can be clearly identified that the total number of modules of such kind of array comes out to be 81. The nomenclature for each module is being clearly laid so that each module is unique and discoverable. If we generalize the module subscript by "mn", where "n" denotes the column and "m" denotes the row at which the module is located. For instance, a module with subscript "92" means, it is located at 2^{nd} column with 9^{th} row in the PVA.

3.2 TCT Configured Photovoltaic Array

There are pros and cons with TCT configuration under PSCs when we compare with the other traditional schemes like SP, BL and HC configurations. The major drawback is that in TCT the physical locations of the entire array and the electrical connections given to those arrays are exactly the same (28 and 31). As a result, the whole array will suffer non-uniform dispersion of shadow. Hence, the row currents will be somewhat more in some rows and less in some rows. That means the row currents are diversified depending upon the strength of solar intensity or irradiance level. In order to protect the modules from severe issues of getting damage due to very less value of row currents, the modules are bypassed. But the difference between maximum power before partial shading and after partial shading increases if the modules are bypassed, i.e. mismatch losses rise in proportion with the number of modules bypassed. Also the number of dips is more in the voltage-current graph. As we increase the voltage, the current is stepped more in the voltage-current graph. Figure.3 inculcates the structure of TCT module with the normal position of modules.

11	**12**	**13**	**14**	**15**	**16**	**17**	**18**	**19**
21	**22**	**23**	**24**	**25**	**26**	**27**	**28**	**29**
31	**32**	**33**	**34**	**35**	**36**	**37**	**38**	**39**
41	**42**	**43**	**44**	**45**	**46**	**47**	**48**	**49**
51	**52**	**53**	**54**	**55**	**56**	**57**	**58**	**59**
61	**62**	**63**	**64**	**65**	**66**	**67**	**68**	**69**
71	**72**	**73**	**74**	**75**	**76**	**77**	**78**	**79**
81	**82**	**83**	**84**	**85**	**86**	**87**	**88**	**89**
91	**92**	**93**	**94**	**95**	**96**	**97**	**98**	**99**

Fig.3 TCT Module arrangement

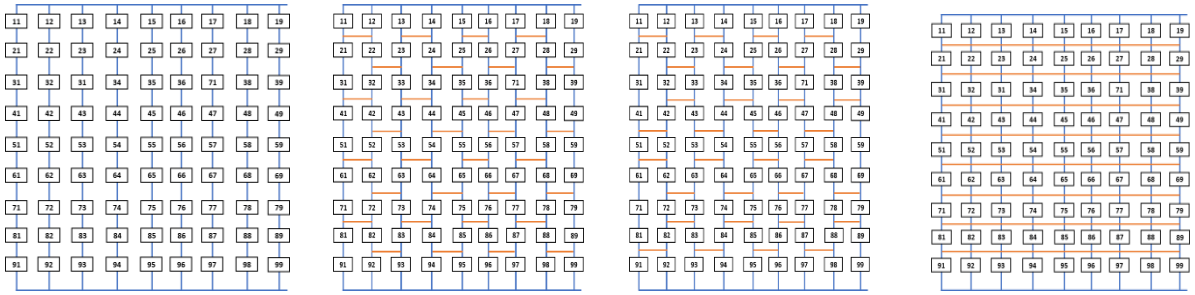

Fig.2 Traditionally configured PVA: (a) SP, (b) BL, (c) HC and (d) TCT

3.3 Methodology- SDT (Shaded Dispersed Topology)

Figure.4 inculcates a novel puzzle structure in which the modules statically reconfigure to adjust their position and eliminate the problem of bypassing and other related issues. The positions of PV modules in TCT configuration align with the novel puzzle configuration. As a result shading is dispersed over the entire array and it is known as shaded dispersed topology (SDT).

The SDT puzzle is a logical placement of numbers. It is of Z×Z size, where Z is any natural number. The SDT puzzle consists of Z rows and Z columns where the rows and columns have the range from 1 to Z without any recurrence. In this paper, we have taken Z=9, i.e. 9×9 PVA. A novel SDT puzzle is used for this research as shown in Figure.4. The first numeral in every module designates the row and the later numeral designates the column. Now, if the modules in TCT topology change their position as per the novel SDT puzzle, then the novel SDT will have efficient output. The most important point is that modules change their position without changing electrical connection, for example, as shown in Figure.4, module 96 is shuffled to new position of row number 7 and column number 6 irrespective of the connection which is at row number 9 and column number 6.

The practice for changing the position of modules is based on the concept of fixing the columns and variation of rows without changing any electrical connection. Hence, the governing equations or relations for TCT topology are valid for novel SDT. As a result the shadow focussing on a one particular region will scatter over the entire module in SDT which reduces the bypassing problem in the modules. The junction current during PSC will also increase under this scheme of novel SDT. Hence, enormous amount of power is generated in SDT in comparison with TCT topology.

21	**42**	**63**	**84**	**15**	**36**	**57**	**78**	**99**
31	**52**	**73**	**94**	**25**	**46**	**67**	**88**	**19**
41	**62**	**83**	**14**	**35**	**56**	**77**	**98**	**29**
51	**72**	**93**	**24**	**45**	**66**	**87**	**18**	**39**
61	**82**	**13**	**34**	**55**	**76**	**97**	**28**	**49**
71	**92**	**23**	**44**	**65**	**86**	**17**	**38**	**59**
81	**12**	**33**	**54**	**75**	**96**	**27**	**48**	**69**
91	**22**	**43**	**64**	**85**	**16**	**37**	**58**	**79**
11	**32**	**53**	**74**	**95**	**26**	**47**	**68**	**89**

Fig.4 Novel SDT configured PVA: Module arrangement

3.3.1 Solving methodology

The backtracking process or algorithm (32 and 33) helps to develop and verify the logic for any puzzle and based on it module arrangement can be established. This algorithm is very useful in finding out unique solution under the situation of tedious calculations. It is often employed when some condition needs to be satisfied. Randomly all the cells are filled one by one until a particular condition is contradicted and when we reach the last cell, a unique solution needs to be claimed which is called 'mandatory' entry. The mock program employed for backtracking process is underlined below:

START

Select the size of PVA

Initialize Array size (A_S) =9, row (i) =1, column (j) =1

if (j=1 and i=i+1)

if ($i \le i_{max}$) {

i=i

}

else i = i-i_{max}

else i=i+1+(j-1)floor($\frac{As}{4}$)

if ($i \le i_{max}$) {

i=i

}

else i = i-i_{max}

if ($j \le j_{max}$) {

j=j

}

else

STOP

4. Performance elements under partial shading scenario

This research focuses on quad core significant elements or factors that will judge the accuracy of 9×9 PVA under partial shading scenario. These significant elements or factors are FF, MP loss and efficiency.

The PV characteristic shows multiple peak points for a PV module under the conditions of partial shading. Fill factor (FF) is a ratio of power under partial shading conditions (global peak power point (GPPP) is achieved corresponding to peak voltage V_{ppp} and peak current I_{ppp}) to the power of ideal source which is without shading (peak point is achieved corresponding to open circuit voltage V_{oc} and short circuit current I_{sc}) (28).

$$FF=\frac{Vppp\times Ippp}{Voc\times Isc} \quad (2)$$

Mismatch power (MP) loss is given by:

$$MP\ loss=P_{ppp}-P_{ppp,psc} \quad (3)$$

Here, P_{ppp} denotes power of ideal source without any shading and $P_{ppp,psc}$ denotes power under partial shading condition. Efficiency is the ratio of output power under partial shading condition to the available input solar power.

5. Results and Discussion

This paper focuses on a novel PVA configuration based on SDT arrangement. The most significant aspect of above arrangement is to get better maximum power output under partial shading conditions. The performance elements are compared among each of the configurations of the SP, BL, HC, TCT and SDT arrangements. Figure.5 is depicting GPPP under the conditions of partial shading.

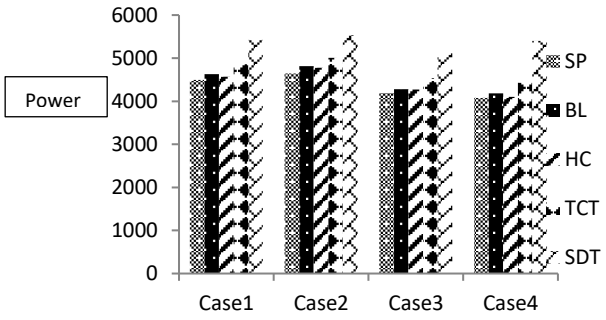

Fig.5 GPPP under conditions of partial shading

Case1: In this case, extreme lower right corner of the PVA is being taken and two different levels of irradiance on the said portion is being incorporated. The two irradiance levels are 200 $\frac{W}{m^2}$ and 800 $\frac{W}{m^2}$. These irradiance levels incorporated on the said portion of the

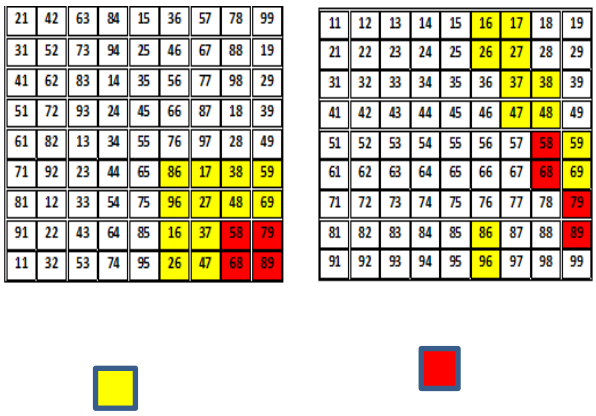

PVA is shown in Figure.6.

200 $\frac{W}{m^2}$ (a) 800 $\frac{W}{m^2}$ (b)

iii **Fig. 6 Case 1 shading: (a) Proposed novel PV array an and (b) SDT**

The currents in the first row for TCT arrangement can be algebraically written as:

$IR_k = J_{k1}I_{k1} + J_{k2}I_{k2} + J_{k3}I_{k3} + J_{k4}I_{k4} + J_{k5}I_{k5} + J_{k6}I_{k6} + J_{k7}I_{k7} + J_{k8}I_{k8} + J_{k9}I_{k9}$ (4)

Where, k = row number

In Eq. (4), $J_{kc} = (S_{kc}/S_{stc})$, where, c = column number and S_{stc} = full irradiance (1000 $\frac{W}{m^2}$)

In full irradiance condition, $S_{kc} = S_{stc}$

Let I_m = Maximum limiting current for full irradiance at STC (25°C, 1000 $\frac{W}{m^2}$), then

currents in first 5 rows will be same with full irradiance levels given by:

$IR_1 = IR_2 = IR_3 = IR_4 = IR_5 = 9I_m$ (5)

Similarly,

$$\begin{cases} IR_6 = IR_7 = 5I_m + 4 \times 0.2I_m = 5.8I_m \\ IR_8 = IR_9 = 5I_m + 2 \times 0.2I_m + 2 \times 0.8I_m = 7I_m \end{cases} \quad (6)$$

The array voltage can be calculated based on the assumption that no row is bypassed and is given by:

$V_{arrray} = 9V_m$ (7)

The array power output with zero shading conditions can be written as:

$P_{arrray} = 9V_mI_m$ (8)

The currents in the various rows for of SDT arrangement for Fig. 6(b) can be algebraically written as:

$$IR_1 = IR_2 = IR_3 = IR_4 = 7I_m + 2 \times 0.2I_m = 7.4I_m \quad (9)$$

Similarly,

$$\begin{cases} IR_5 = IR_6 = IR_8 = 7I_m + 0.2I_m + 0.8I_m = 8I_m \\ IR_7 = 8I_m + 0.8I_m = 8.8I_m \end{cases} \quad (10)$$

And $IR_9 = 8I_m + 0.2I_m = 8.2I_m$ (11)

In case of TCT topology, it can be observed that peak power can be attained when the bottom four rows get bypassed. The peak power of TCT topology in this case is 4595.7 W. The position of GPPP is at a point below the normal conditions (no shading). The results are verified using the SIMULINK/MATLAB software and compared with the theoretical aspects. The voltage under GPPP is 195.4 V. The P-V characteristic and V-I characteristic for case 1 is depicted in Figure.7 and Figure.8.

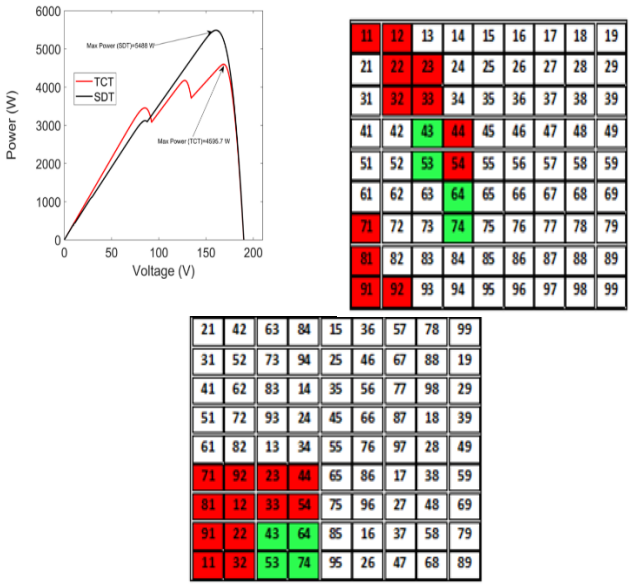

Fig. 7 Case 1 simulation results: P-V characteristic

The conclusion which can be made here is that GPPP for TCT topology is 4595.7 W while that of SDT is 5488 W. This value in case of SDT is greater than TCT topology by 16.259%.

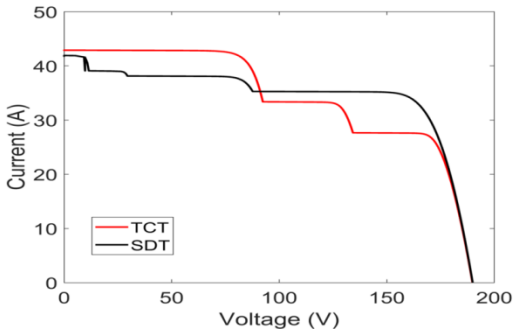

Fig. 8 Case 1 simulation results: V-I characteristic

The significant observation which can be made from case1 is that the power losses are comparatively lower in SDT as compared to conventional TCT topology. It can be clearly revealed from Figure.5 and Figure.9 that the significant parameters like GPPP, FF, MP loss and efficiency are optimum for SDT as compared with conventional topologies.

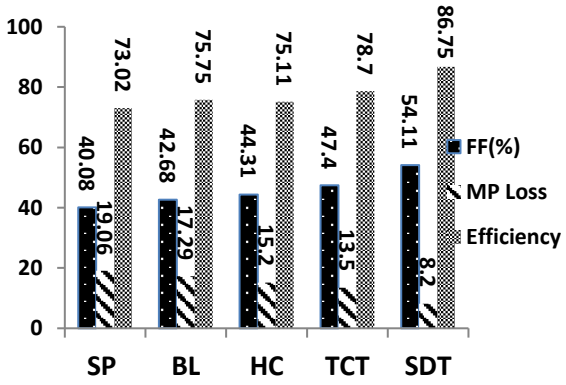

Fig. 9 FF, MP Loss and efficiency for first case

Case 2: In this case, extreme lower left corner of the PVA is being taken and two different levels of irradiance on the said portion is being incorporated. The two irradiance levels are 800 $\frac{W}{m^2}$ and 500 $\frac{W}{m^2}$. These irradiance levels incorporated on the said portion of the PVA is shown in Figure.10.

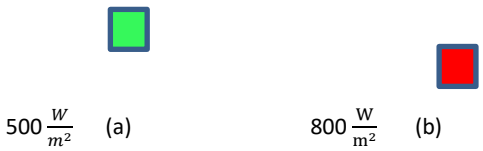

500 $\frac{W}{m^2}$ (a) 800 $\frac{W}{m^2}$ (b)

Fig. 10 Case 2 shading: (a) Proposed novel PV array and (b) SDT

The currents in first 5 rows will be same with full irradiance levels given by:

$IR_1 = IR_2 = IR_3 = IR_4 = IR_5 = 9I_m$ (12)

Similarly,

$$\begin{cases} IR_6 = IR_7 = 5I_m + 4 \times 0.8I_m = 8.2I_m \\ IR_8 = IR_9 = 5I_m + 2 \times 0.5I_m + 2 \times 0.8I_m = 7.6I_m \end{cases} \quad (13)$$

The currents in the various rows for of SDT arrangement for Fig. 10(b) can be algebraically written as:

$$IR_1 = IR_2 = IR_3 = IR_9 = 7I_m + 2 \times 0.8I_m = 8.6I_m \quad (14)$$

Similarly,

$$\begin{cases} IR_4 = IR_5 = IR_7 = 7I_m + 0.5I_m + 0.8I_m = 8.3I_m \\ IR_8 = 8I_m + 0.8I_m = 8.8I_m \end{cases} \quad (15)$$

And $IR_6 = 8I_m + 0.5I_m = 8.5I_m$ (16)

In case of TCT topology, it can be observed that peak power can be attained when the bottom four rows get bypassed. The peak power of TCT topology in this case is 5821.1 W. The position of GPPP is at a point below the normal conditions (no shading). The results are verified using the SIMULINK/MATLAB software and compared with the theoretical aspects. The voltage under GPPP is 189.5 V. The P-V characteristic and V-I characteristic for case 2 is depicted in Figure.11 and Figure.12.

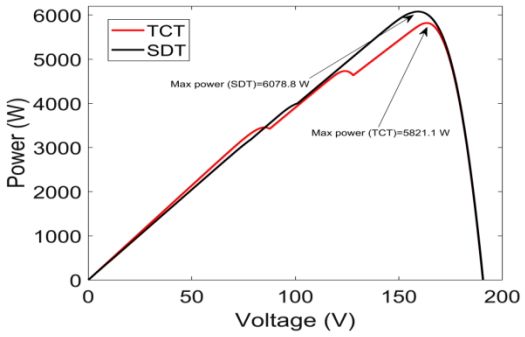

Fig. 11 Case 2 simulation results: P-V characteristic

The conclusion which can be made here is that GPPP for TCT topology is 5821.1W while that of SDT is 6078.8 W. This value in case of SDT is greater than TCT topology by 4.239%.

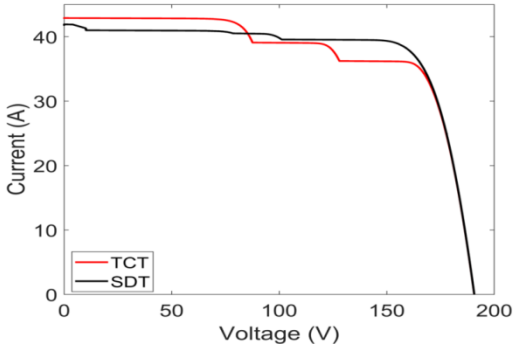

Fig. 12 Case 2 simulation results: V-I characteristic

The significant observation which can be made from case1 is that the power losses are comparatively lower in SDT as compared to conventional TCT topology. It can be clearly revealed from Figure.13 that the significant parameters like FF, MP loss and efficiency are optimum for SDT as compared with conventional topologies.

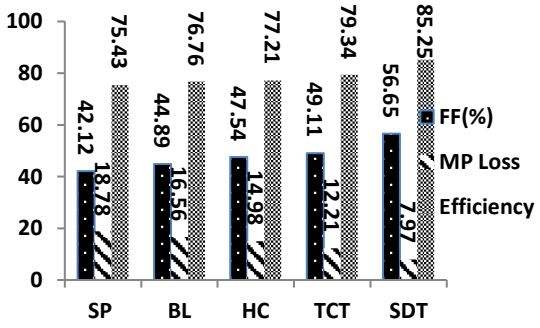

Fig. 13 FF, MP Loss and efficiency for second case

Case 3: In this case, extreme upper left corner of the PVA is being taken and two different levels of irradiance on the said portion is being incorporated. The two irradiance levels are 200 $\frac{W}{m^2}$ and 300 $\frac{\mathrm{W}}{\mathrm{m}^2}$. These irradiance levels incorporated on the said portion of the PVA is shown in Figure.14.

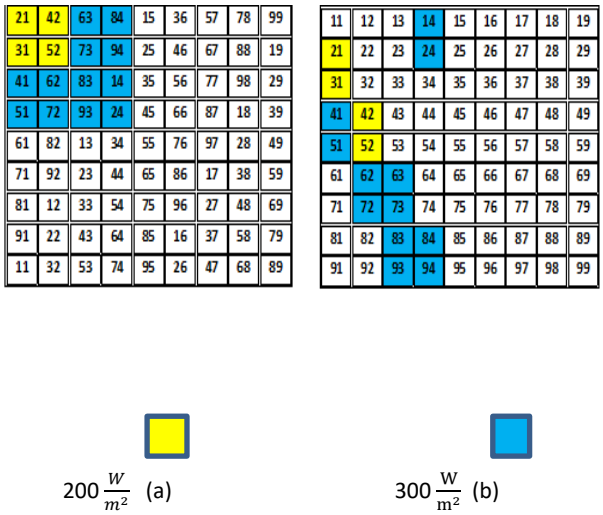

Fig. 14 Case 3 shading: (a) Proposed novel PV array and (b) SDT

The currents in last 5 rows will be same with full irradiance levels given by:

$$IR_5 = IR_6 = IR_7 = IR_8 = IR_9 = 9I_m \quad (17)$$

Similarly,

$$\begin{cases} IR_3 = IR_4 = 5I_m + 4 \times 0.3I_m = 6.2I_m \\ IR_1 = IR_2 = 5I_m + 2 \times 0.2I_m + 2 \times 0.3I_m = 6I_m \end{cases} \quad (18)$$

The currents in the various rows for of SDT arrangement for Fig. 14(b) can be algebraically written as:

$$IR_6 = IR_7 = IR_8 = IR_9 = 7I_m + 2 \times 0.3I_m = 7.6I_m \quad (19)$$

Similarly,

$$\begin{cases} IR_4 = IR_5 = IR_2 = 7I_m + 0.2I_m + 0.3I_m = 7.5I_m \\ IR_1 = 8I_m + 0.3I_m = 8.3I_m \end{cases} \quad (20)$$

And $IR_3 = 8I_m + 0.2I_m = 8.2I_m$ (21)

In case of TCT topology, it can be observed that peak power can be attained when the upper four rows get bypassed. The peak power of TCT topology in this case is 4666.2 W. The position of GPPP is at a point below the normal conditions (no shading). The results are verified

using the SIMULINK/MATLAB software and compared with the theoretical aspects. The voltage under GPPP is 184.4 V. The P-V characteristic and V-I characteristic for case 3 is depicted in Figure.15 and Figure.16.

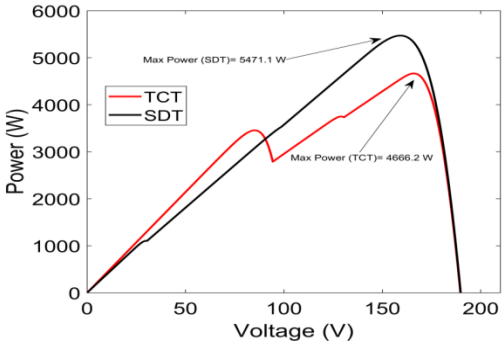

Fig. 15 Case 3 simulation results: P-V characteristic

The conclusion which can be made here is that GPPP for TCT topology is 4666.2 W while that of SDT is 5471.1 W. This value in case of SDT is greater than TCT topology by 14.711%.

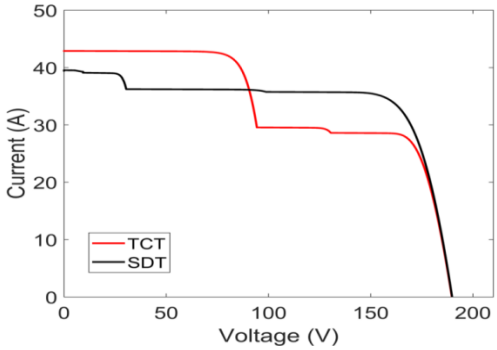

Fig. 16 Case 3 simulation results: V-I characteristic

The significant observation which can be made from case3 is that the power losses are comparatively lower in SDT as compared to conventional TCT topology. It can be clearly revealed from Figure.17 that the significant parameters like FF, MP loss and efficiency are optimum for SDT as compared with conventional topologies.

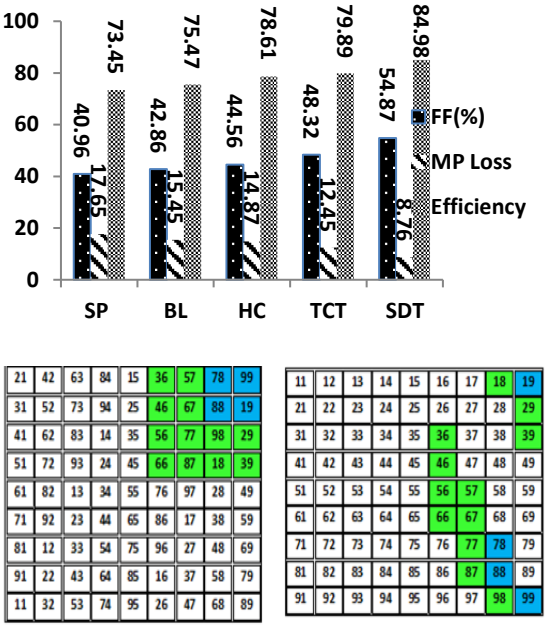

Fig. 17 FF, MP Loss and efficiency for third case

Case 4: In this case, extreme upper right corner of the PVA is being taken and two different levels of irradiance on the said portion is being incorporated. The two irradiance levels are 500 $\frac{W}{m^2}$ and 300 $\frac{\mathrm{W}}{\mathrm{m}^2}$. These irradiance levels incorporated on the said portion of the PVA is shown in Figure.18.

500 $\frac{W}{m^2}$ (a)

300 $\frac{\mathrm{W}}{\mathrm{m}^2}$ (b)

Fig. 18 Case 4 shading: (a) Proposed novel PV array and (b) SDT

The currents in last 5 rows will be same with full irradiance levels given by:

$$IR_5 = IR_6 = IR_7 = IR_8 = IR_9 = 9I_m \quad (22)$$

Similarly,

$$\begin{cases} IR_3 = IR_4 = 5I_m + 4 \times 0.5I_m = 7I_m \\ IR_1 = IR_2 = 5I_m + 2 \times 0.5I_m + 2 \times 0.3I_m = 6.6I_m \end{cases}$$

(23)

The currents in the various rows for of SDT arrangement for Fig. 18(b) can be algebraically written as: $IR_3 = IR_5 = IR_6 = 7I_m + 2 \times 0.5I_m = 8I_m$ (24)

Similarly,

$$\begin{cases} IR_1 = IR_7 = IR_8 = IR_9 = 7I_m + 0.3I_m + 0.5I_m = 7.8I_m \\ IR_2 = IR_4 = 8I_m + 0.5I_m = 8.5I_m \end{cases}$$

(25)

In case of TCT topology, it can be observed that peak power can be attained when the bottom four rows get bypassed. The peak power of TCT topology in this case is 5124 W. The position of GPPP is at a point below the normal conditions (no shading). The results are verified using the SIMULINK/MATLAB software and compared with the theoretical aspects. The voltage under GPPP is 187.8 V. The P-V characteristic and V-I characteristic for case 4 is depicted in Figure.19 and Figure.20.

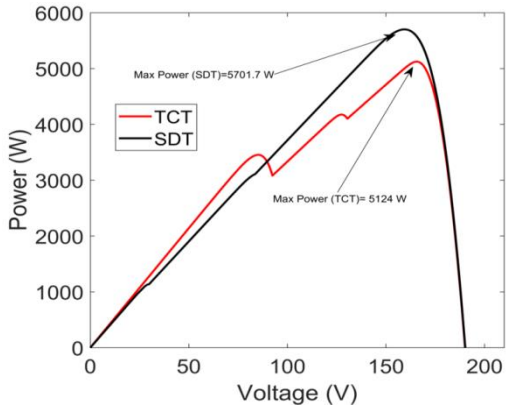

Fig. 19 Case 4 simulation results: P-V characteristic

The conclusion which can be made here is that GPPP for TCT topology is 5124 W while that of SDT is 5701.7 W. This value in case of SDT is greater than TCT topology by 10.132%.

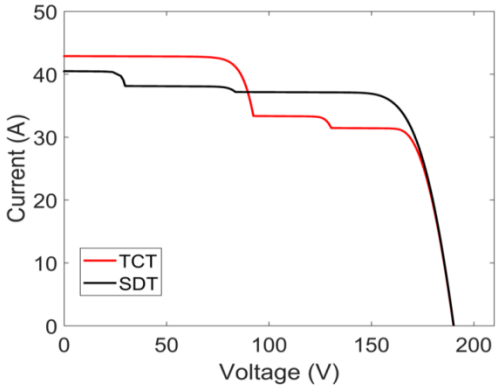

Fig. 20 Case 4 simulation results: V-I characteristic

The significant observation which can be made from case1 is that the power losses are comparatively lower in SDT as compared to conventional TCT topology. It can be clearly revealed from Figure.21 that the significant parameters like FF, MP loss and efficiency are optimum for SDT as compared with conventional topologies.

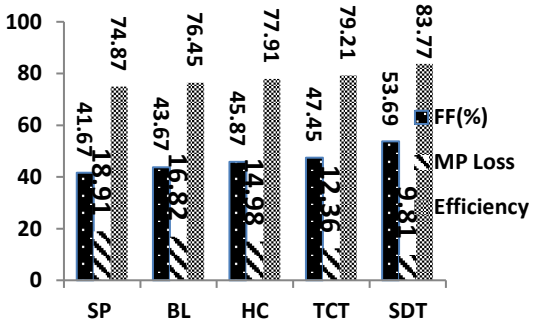

Fig. 21 FF, MP Loss and efficiency for fourth case

6. Conclusion and Scope of Future Work

This article presents a careful and detailed examination of the SP, TCT, HC, TCT, and SDT rearrangement patterns in a 9 × 9 PVA. All these PVACs are evaluated and contrasted based on specific intrinsic criteria, such as measured voltage, current, power at GPPP, MP loss, fill factor (FF), and efficiency. Besides these factors, the influence of shade dispersion on the presented configuration is also examined. Extensive simulations have been conducted considering all these factors and

the in-depth examination of the results indicates that the HS reconfiguration pattern corresponds to minimal power losses, improved fill factor (FF), and enhanced efficiency in diverse shading situations.

Looking ahead, larger-capacity PV plants could be developed using a 9 × 9 TCT PVAC, with each module potentially substituted by a 9 × 9 SDT PVAC. Hence, the suggested SDT method warrants additional exploration as the optimal reconfiguration strategy involving physical relocation for expansive solar power facilities.

Abbreviations

SDT: Shaded Dispersed Topology, TCT: Total Cross-Tied, FF: Fill Factor, MP Loss: Mismatch Power Loss, PSC: Partial Shading condition, GPPP: Global Peak Power Point, PVA: Photovoltaic Array

Acknowledgment

The authors would like to thank Integral University, Lucknow for providing manuscript communication number IU/R&D/2025-MCN0003913 and necessary support for the research.

References

[1] Y. Zhao, "A review of renewable energy and power system integration," *Applied and Computational Engineering,* vol. 126, pp. 112–128, Jan. 2025.

[2] V. K. Sharma, G. Monteleone, G. Braccio, C. N. Anyanwu, and N. N. Aneke, "A comprehensive review of green energy technologies: Towards sustainable clean energy transition and global net-zero carbon emissions," *Processes*, vol. 13, no. 1, pp. 69–98, Dec. 2024.

[3] S. S. Dol, A. H. M. Amin, and H. Hamdan, "Advances in renewable energy research and applications," *Energies*, vol. 17, no. 23, pp. 6198–6215, Dec. 2024.

[4] A. Ali, M. Zubair, A. Waseem, M. Asim, M. T. Khan, and S. Rehman, "A review of partial shading impact on photovoltaic systems: Effects, mitigation techniques, and future directions," *Solar Energy*, vol. 268, pp. 112–131, Feb. 2025.

[5] R. Kumar, P. S. Babu, and M. S. Bhaskar, "Performance evaluation of PV modules under partial shading conditions caused by dynamic environmental factors," *Renewable Energy*, vol. 220, pp. 845–859, Jan. 2025.

[6] V. Jha, "Analysis of the performances of dissimilar PV array topologies under realistic partial shading condition," *Journal of the Institution of Engineers (India): Series B*, vol. 105, no. 10, pp. 1169–1181, Oct. 2024.

[7] V. A. Potnuru, S. Iysaouy, A. Chalco, and S. Al-Ezzi, "A MATLAB-based modelling to study and enhance the performance of photovoltaic panel configurations during partial shading conditions," *Frontiers in Energy Research*, vol. 11, pp. 1–15, May 2023.

[8] M. Abdel-Salam, R. K. Saket, and H. Elgamal, "Global maximum power point tracking techniques for photovoltaic systems under partial shading: A review," *Solar Energy*, vol. 247, pp. 340–358, Apr. 2023.

[9] N. Patel, A. K. Yadav, and R. Singh, "A hybrid bio-inspired MPPT approach for accurate GMPP detection in PV systems with multiple peaks," *Renewable Energy*, vol. 210, pp. 512–526, Nov. 2023.

[10] S. Patel, M. Pathak, and V. Agarwal, "Comprehensive review of PV array configurations under partial shading: Performance evaluation and loss mitigation," *Solar Energy*, vol. 243, pp. 320–338, Jan. 2023.

[11] R. Ranjan, P. K. Sahoo, and S. Mishra, "Performance analysis of series, series-parallel, total cross-tied, bridge-linked, and honey-comb PV array topologies under different shading patterns," *Renewable Energy*, vol. 215, pp. 654–670, Feb. 2024.

[12] A. Khan, S. Sharma, and R. Gupta, "Comparative analysis of photovoltaic array configurations under various partial shading patterns," *Solar Energy*, vol. 256, pp. 745–761, Aug. 2023.

[13] P. Verma, D. Chaturvedi, and A. Kumar, "Modeling and performance evaluation of series, parallel, TCT, BL, HC, and SP PV array topologies under dynamic shading conditions," *Renewable Energy*, vol. 222, pp. 1180–1196, Mar. 2024.

[14] S. Banerjee, M. Singh, and A. Rathore, "Evaluation of total cross-tied PV array configuration under non-uniform irradiance: Benefits and limitations," *Solar Energy*, vol. 259, pp. 215–229, Oct. 2023.

[15] K. R. Bansal, P. Mehta, and R. Agarwal, "Reconfiguration strategies for total cross-tied photovoltaic arrays under partial shading to minimize mismatch power loss," *Renewable Energy*, vol. 228, pp. 940–955, Apr. 2024.

[16] A. Kumar, S. R. Patel, and M. Chauhan, "Dynamic reconfiguration of photovoltaic arrays using irradiance-dependent controller for enhanced performance under partial shading," *Solar Energy*, vol. 261, pp. 482–495, Dec. 2023.

[17] L. Singh, V. Yadav, and R. K. Misra, "Fuzzy logic-based controller for dynamic PV array selection under variable irradiance conditions," *Renewable Energy*, vol. 216, pp. 410–423, Mar. 2023.

[18] P. Joshi and A. K. Sharma, "Rule-based PV array configuration using irradiance level mapping for

improved performance under partial shading," *Solar Energy*, vol. 262, pp. 705–718, Jan. 2024.

[19] H. Chen, M. Zhao, and Y. Li, "Commercial-scale PV array system design and energy distribution performance analysis," *Energy Reports*, vol. 10, pp. 2331–2345, Nov. 2024.

[20] S. Gupta, A. Rawat, and D. K. Jain, "Optimized reconfiguration algorithm for photovoltaic arrays under partial shading using module relocation techniques," *IEEE Access*, vol. 12, pp. 54120–54134, Jun. 2024.

[21] M. R. Alam, K. K. Tiwari, and S. K. Panigrahi, "A novel PV array reconfiguration algorithm to mitigate shading effects and enhance power output," *Solar Energy*, vol. 257, pp. 621–635, Sep. 2023.

[22] F. Rahman, Z. Hussain, and A. Ahmad, "Variable switching state strategy for photovoltaic arrays under partial shading to achieve row-current independence," *Renewable Energy*, vol. 223, pp. 1197–1210, Apr. 2024.

[23] J. Mehta, V. Chauhan, and D. Sharma, "Dynamic reconfiguration of PV arrays under shading and fault conditions: Performance enhancement versus complexity trade-offs," *IEEE Transactions on Sustainable Energy*, vol. 15, no. 2, pp. 1180–1192, Feb. 2024.

[24] A. Sharma, P. K. Yadav, and R. Patel, "Curved photovoltaic array reconfiguration for enhanced power extraction under partial shading," *Renewable Energy*, vol. 210, pp. 945–958, Jan. 2023.

[25] S. K. Singh, D. Bansal, and H. Choudhary, "A novel square third-level schematic photovoltaic array for shading distribution and global maximum power enhancement," *Solar Energy*, vol. 245, pp. 1124–1138, Jul. 2022.

[26] M. Verma, A. Thakur, and V. Kumar, "Magical-rhombus photovoltaic array reconfiguration to minimize mismatch loss and maximize power under shading," *International Journal of Photoenergy*, vol. 2023, pp. 1–14, Article ID 8856342, 2023.

[27] K. Gupta, S. P. Singh, and R. Chauhan, "Performance improvement of photovoltaic arrays under partial shading using twin dispersed reconfiguration," *IEEE Journal of Photovoltaics*, vol. 14, no. 1, pp. 278–287, Jan. 2024.

[28] R. N. Patel, S. K. Mishra, and V. P. Singh, "Puzzle-based total-cross-tied photovoltaic array reconfiguration for improved global maximum power and fill factor under partial shading," *Solar Energy*, vol. 256, pp. 312–325, Sept. 2023.

[29] M. A. Khan, T. S. Babu, and B. K. Panigrahi, "Performance assessment of large-scale 9 × 9 total-cross-tied photovoltaic array configurations under diverse shading conditions," *Renewable Energy*, vol. 195, pp. 586–598, Oct. 2022.

[30] Asim M, Sarwar A, Shahabuddin M, Manzar M.S, 2021, Development of solar photovoltaic model for wide range of operating conditions, International Journal of Power Electronics and Drive Systems (IJPEDS), 12:4, 2483-2491.

[31] Khatri K, Shadab M.M, Shadab, 2023, Windoku Based Solar PV Array One Time Reconfiguration for Maximum Power Enhancement under Partial Shading Scenarios 2023 International Conference on Power, Instrumentation, Energy and Control (PIECON), 979-8-3503-9977-6.

[32] S. R. Sharma and K. Rajasekar, "Application of backtracking algorithm for puzzle-based photovoltaic array reconfiguration under partial shading conditions," *Energy Conversion and Management*, vol. 287, pp. 117040–117052, Apr. 2023.

[33] Uvais M, Ansari A.J, Asim, M, Manzar M.S, 2024, Optimized parameter extraction techniques for enhanced performance evaluation of organic solar cells, International Journal of Electrical and Computer Engineering (IJECE), 14:2, 1263-1273.